

Extreme Adaptive Optics using an off-axis subaperture on a ground-based telescope

E. Serabyn, J.K. Wallace, M. Troy, B. Mennesson, P. Haguenaer, R.O. Gappinger, E.E. Bloemhof
Jet Propulsion Laboratory, California Institute of Technology,
4800 Oak Grove Drive, Pasadena, CA, USA 91109

ABSTRACT

The next generation of adaptive optics (AO) systems, often referred to as extreme adaptive optics (ExAO), will use higher numbers of actuators to achieve wavefront correction levels below 100 nm, and so enable a host of new observations such as high-contrast coronagraphy. However, the number of potential coronagraph types is increasing rapidly, and selection of the most advantageous coronagraph is subject to many factors. Here it is pointed out that experiments in the ExAO regime can already be carried out with existing hardware, by using a well-corrected subaperture on an existing telescope. For example, by magnifying a 1.5 m diameter off-axis subaperture onto the AO system's deformable mirror (DM) on the Palomar Hale telescope, we have recently achieved stellar Strehl ratios as high as 92% to 94%, corresponding to wavefront errors of 85 - 100 nm. Using this approach, a wide variety of ExAO experiments can thus be carried out well before "next generation" ExAO systems are deployed on large telescopes. The potential experiments include infrared ExAO imaging and performance optimization, a comparison of coronagraphic approaches in the ExAO regime, visible wavelength AO, and predictive AO.

Keywords: Extreme adaptive optics

1. INTRODUCTION

The direct detection of very faint companions close to much brighter stars requires very high-contrast observations at small angular separations. Coronagraphic starlight suppression techniques show great promise in this regard, but observations with classical "Lyot" coronagraphs (using opaque blockers in the image plane) are limited by a number of factors, among them reduced throughput and a large central exclusion zone, or inner working angle (IWA). As a result, a number of novel coronagraphic approaches have recently been proposed (e.g., Guyon, this conf.). However, for any coronagraphic technique, the suppression of scattered stellar light remains paramount, as the performance is ultimately determined by the achievable wavefront correction level¹. In particular, for ground-based telescopes, practical inner working angles are typically significantly larger than theoretical limits, due to the detrimental effects of wavefront errors, and classical coronagraphs do not seem to provide significant contrast improvement² for Strehl ratios below 90%.

The main current limitation to coronagraphic observations on ground-based telescopes is thus the corrected wavefront quality provided by the AO system. Both scattering from wavefront phase errors and from pupil obstructions degrade the image quality. As we point out here, one way of obtaining a highly corrected wavefront is simply to use an existing wavefront sensor (WFS) and DM to more finely sample and correct a sub-aperture smaller than the full telescope pupil. In this case, the reduced corrector spacing should lead to significantly smaller wavefront errors within the sub-pupil. However, imaging performance is in general also degraded by pupil obstructions such as an on-axis secondary mirror and secondary support legs. These blockages can be eliminated by use of a telescope sub-aperture that is unvignetted, i.e., an off-axis subaperture that lies between the secondary support legs. With an unvignetted, off-axis, well-corrected sub-aperture (WCS) a dual image improvement can thus be obtained: scattering due to wavefront aberrations is reduced, and scattering by pupil blockages is also eliminated.

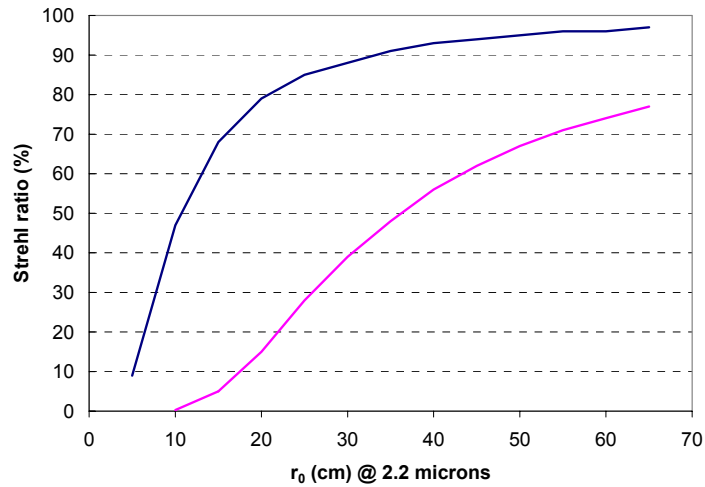


Fig. 1. Comparison of Strehl ratios obtainable with the full Palomar 200 inch telescope (5.08 m diameter; bottom curve) and a sub-aperture of diameter 1.5 m (top curve) for a 16 x 16 element corrector.

The potential level of wavefront improvement with a WCS can be seen in Figure 1, which compares Strehl ratios obtainable for the full aperture and sub-aperture cases for the 200-inch diameter Hale telescope at the Palomar Observatory, as a function of r_0 , the atmospheric seeing cell size. For typical r_0 's of 30 - 50 cm in the K band ($2.2 \mu\text{m}$), residual wavefront errors can be reduced from current levels of 200 - 250 nm to under 100 nm, thus increasing Strehl ratios from about 40-70% to 88-96%. Such performance levels can enable a variety of coronagraphic approaches to be used more effectively. Indeed, as is evident in Figure 2, such high wavefront correction levels can also enable AO observations into the visible domain. Indeed, a wavefront accuracy of about 100 nm would enable AO observations at red wavelengths with Strehl ratios comparable to those obtained at the present time using the full telescope in the infrared.

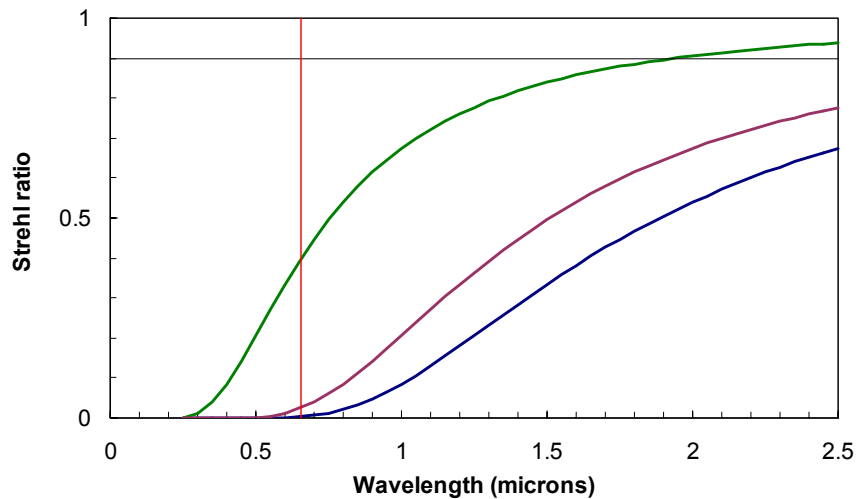


Fig. 2. Strehl ratio vs wavelength for rms wavefront accuracies of 100, 200 and 250 microns (top to bottom). The vertical line shows the wavelength of the $H\alpha$ line, and the horizontal line shows the 90% level at which coronagraphic contrast improvement becomes significant.

Of course with a WCS, the smaller sub-aperture implies lower angular resolution than is possible with the full telescope aperture. This resolution loss is partially offset by the ability to make coronagraphic observations closer to the star (in λ/D units) because of the higher quality wavefront. Moreover, shorter wavelengths can be used to regain angular resolution. Furthermore, some coronagraphs, such as the four-quadrant phase mask (FQPM) coronagraph, in principle have better performance with an unobscured aperture³.

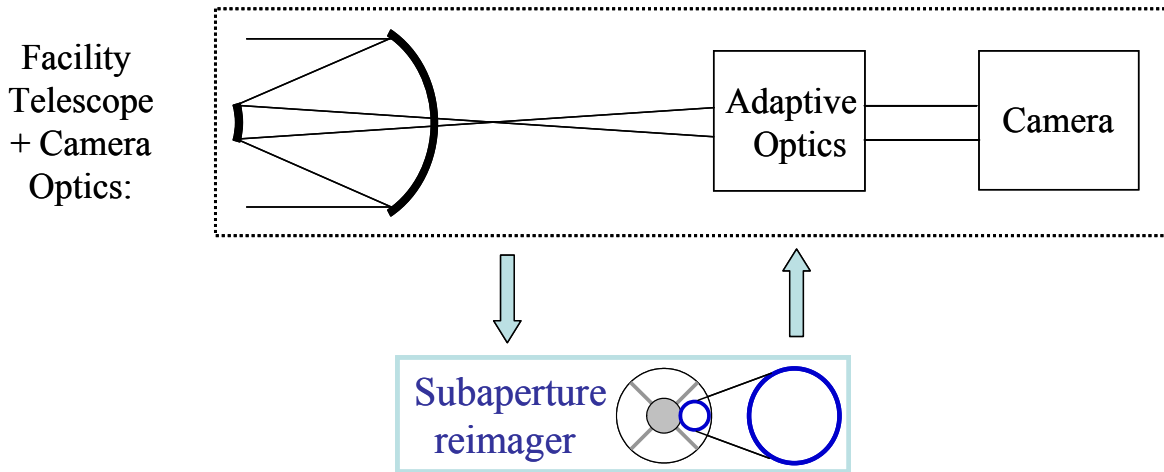


Fig. 3. Block diagram of the optical system for generating a well-corrected subaperture. A set of relay optics is inserted prior to the facility AO system. The relay optics magnify an off-axis subaperture and send it to the DM, while maintaining the pupil location at the DM, and the post-DM F#.

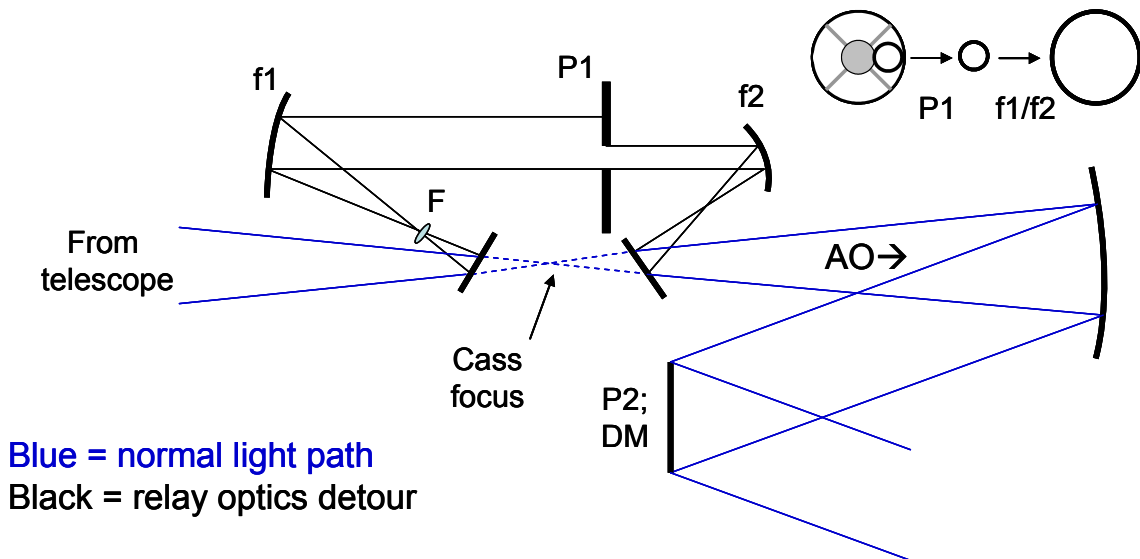


Fig. 4. Conceptual layout of the off-axis relay optics. The incoming beam is first diverted from its original path (dashed) by a fold mirror, and then collimated by an off-axis paraboloid (OAP) f_1 . The field lens F controls the location of the pupil. At the first pupil plane, P_1 , a slightly oversized off-axis subaperture is selected and then a second OAP, f_2 , focuses the sub-aperture beam with the same $F\#$ as the original beam. Finally, a fold mirror restores the beam to its original path to the AO system. This system yields a sub-aperture image expanded by the ratio f_1/f_2 , so as to match the diameter of the DM (the second pupil location, P_2). The true pupil stop is located at the position of the DM.

2. EXPERIMENTAL IMPLEMENTATION

To provide a WCS with ExAO correction levels, all that is needed is a set of relay optics to reimagine the selected subaperture onto the DM. On Palomar's Hale telescope, the maximum possible off-axis pupil diameter is 1.5 m, so a 16 x 16 element corrector can provide an actuator spacing of about 10 cm. The relay optics would need to be inserted upstream of the AO system, as is illustrated in Figure 3, and would need to restore the original beam F# for transmission to the AO system. In this way, neither the AO system, nor the final science camera would notice any illumination differences.

The specific goals for the relay optics system are then to 1) magnify the pupil to the desired scale, 2) maintain the pupil location at the DM, 3) center an off-axis sub-pupil onto the DM, and 4) maintain the post-DM F# to the rest of the AO system. The post-DM optical beam through the rest of the AO system is then unaltered in terms of both F# and pupil location. The science camera then also sees same F# & pupil location and size, implying that the final image of a point source is unchanged in physical scale on the detector array. The only change is then that the plate scale on the sky is demagnified. This demagnification, which results from the conservation of the $A\Omega$ product, comes about by means of a pair of unmatched off-axis paraboloids (OAPs), f_1 and f_2 , in the relay optics. These OAPs magnify the pupil diameter by the ratio of the focal lengths, f_1/f_2 (the pupil is then truncated back to its original diameter at the DM), and demagnify the camera plate scale by the same factor.

The resultant conceptual layout for a set of relay optics which meets all of these goals is shown in Figure 4. In practice, extra fold mirrors are required, and in our case, the field lens is actually a (spherical) mirror rather than a lens. While the real system that we implemented is thus slightly more complicated than that shown in Fig. 4, this figure does capture all of the essential elements.

In early 2005, we installed a set of relay optics following this scheme on the Hale telescope at the Palomar Observatory. The relay optics are all mounted on a small optical bench that is mounted above the Palomar AO bench, PALAO, as is shown in Fig. 5. When the AO bench is mounted on the telescope, the relay optics bench (ROB) is located inside the central hole in the 200 inch primary mirror. To use our relay optics, a small fold mirror on a translation stage can be inserted into the incoming beam to redirect the starlight through our relay optics.

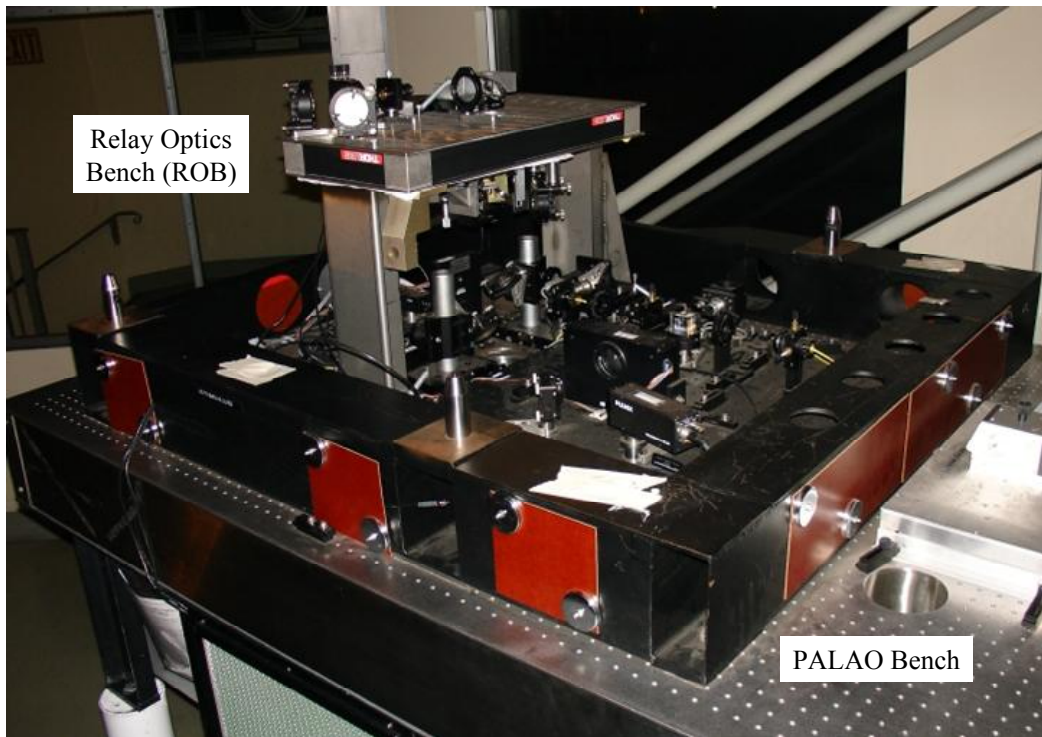


Fig. 5. Our relay optics bench (ROB) mounted on the Palomar Adaptive optics bench (PALAO).

3. INITIAL OBSERVATIONAL RESULTS

Many ExAO experiments are enabled by the high wavefront quality obtainable with a well-corrected sub-aperture. Examples include infrared (IR) ExAO, IR high-contrast coronagraphy, visible wavelength AO, and predictive AO. Initial experiments in the first three of these categories have now been carried out with our off-axis sub-aperture on the Hale telescope, and initial illustrative results are presented in the following sections.

3.1 ExAO infrared wavefront correction

The first test was to image a single star with our WCS to determine image quality. Figure 6 shows one of our best images of the single star HD 121107, obtained in June 2005. The image closely resembles a diffraction-limited Airy pattern, with seven circular Airy rings clearly present. Indeed, bits of rings up to the ninth are also evident, and longer integrations would presumably have revealed even further rings. The image quality is perhaps even slightly better than that of the Hubble Space Telescope's NICMOS camera at the same wavelength, due partially to the unobscured aperture, with Strehl ratios in the 92 – 94% range, corresponding to wavefront errors in the 85 – 100 nm range.

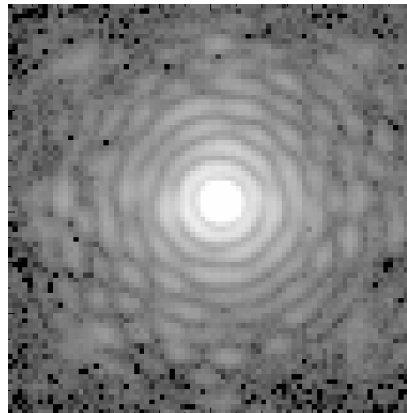


Fig. 6. Image of HD 121107 with our WCS in the 2.17 μ m Br γ filter.

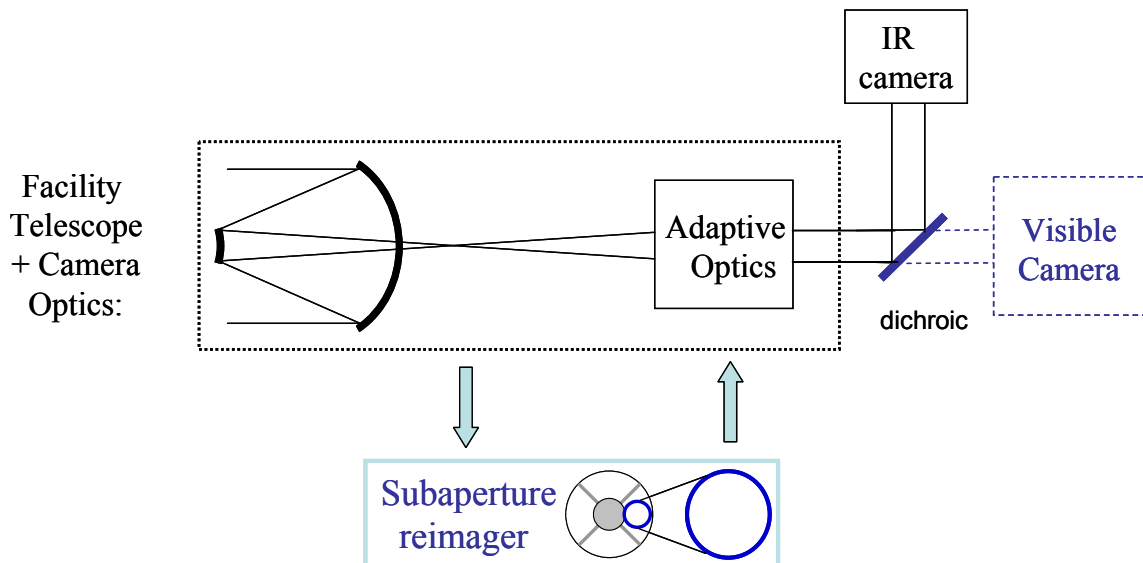


Fig. 7. Layout for visible wavelength AO.

3.2 Visible AO

With such high Strehl ratios, visible AO seemed a distinct possibility with our WCS. To make room for a visible camera in the system, we inserted a dichroic splitter which transmits visible light and reflects the infrared, as in the layout of Fig. 7. Even so, little visible light reaches this camera, because most of the visible passband is extracted by the WFS. However, the WFS dichroic does transmit longward of about $1\ \mu\text{m}$ and shortward of about $450\ \text{nm}$. We thus used an astronomical B-band filter for the initial observations, which yields a passband of roughly $400\text{-}450\ \text{nm}$ after allowing for the effect of the WFS dichroic.

In May 2006 we used a rather basic visible camera to obtain AO-corrected stellar images in the B band with our WCS. Blue images of both single and binary stars were obtained, and these are shown in Figures 8 and 9. For the single star Denebola, we spent a fair amount of time optimizing and removing non-common path defocus and astigmatism errors between the WFS and the visible camera, and the resultant image (Fig. 8) shows the starlight fairly tightly concentrated into a single pixel, with a surrounding halo. Thus, a diffraction-limited core is seen even at these short wavelengths. We also observed the binary SAO 160332 (Figure 9). While this image is less well focused, it clearly shows a pair of well-separated stars. The separation of SAO 160332, $0.59\ \text{arc sec}$ at the time of the observations, is very well resolved by our $\approx 58\ \text{milli arc second}$ beam. Denebola and the pair of stars in SAO 160332 are all rather bright, 2^{nd} to 3^{rd} mag, but with a more sensitive visible camera we can more fully exploit AO-corrected observations at visible wavelengths⁴.

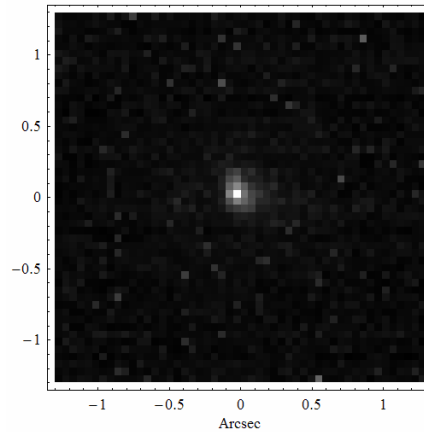


Fig. 8. B band AO-corrected image of the star Denebola with our WCS. The subaperture diffraction FWHM is $\approx 58\ \text{milli arc sec}$, while a single pixel is $53\ \text{milli arc sec}$.



Fig. 9. B-band AO-corrected image of the binary SAO160332, with an intrinsic separation of $0.59\ \text{arc sec}$. The focus and astigmatism have not been optimized for this image.

3.3 IR coronagraphy

We also carried out initial IR coronagraphic observations with our WCS. The coronagraph that we chose to begin with is the FQPM coronagraph^{5,6}, because of its need for an unobscured circular aperture. Our coronagraphic measurements are described in more detail elsewhere⁷⁻⁹, but here a quick overview is provided. Figure 10 shows our observations of the binary HD 148112 in June 2005: the left-hand panel shows the normal “off-coronagraph” image, the central panel shows the “through-FQPM” image, and the right-hand panel shows the through-FQPM image after cross-diagonal subtraction. After passage through the coronagraph, the fainter (by a factor of 23) companion at $\approx 2\lambda/D$ emerges as the brightest source in the field by a factor of 10.

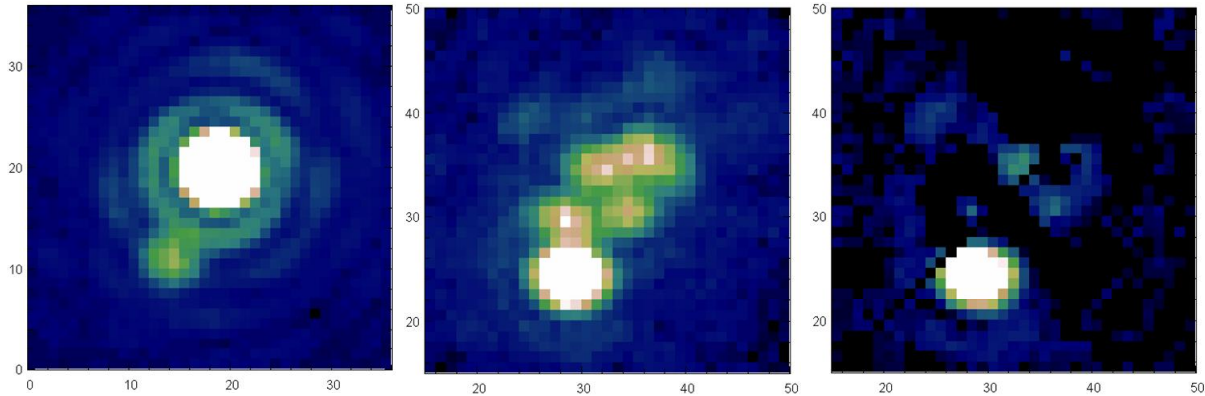


Fig. 10. Observations of the binary HD 148112 in the narrowband Br γ filter with our Palomar WCS. Left: normal (without FQPM) image. Center: through-FQPM image. Right: cross-diagonal subtraction of through-FQPM image. The highest residual peak is down by 235:1.

More recently, we imaged a higher contrast target. Figure 11 shows our recent (May 2006) observations of HD130948. For these observations, we used the entire K_s band so as to reach better sensitivity levels. The faint brown dwarf (unresolved) pair is clearly present at about 10 o'clock in the image. The position of the faint companion (which is itself an unresolved pair) agrees well with the initial discovery image obtained with the 8 m Gemini telescope¹⁰. The contrast ratio between the primary and the unresolved binary is measured to be 6.9 mag in the K_s filter, and it is clear from the image that this brown dwarf could have been detected at a radial offset half as large as it is in reality. Detections at even smaller radial offsets and higher contrasts should thus be possible with improved phase masks.

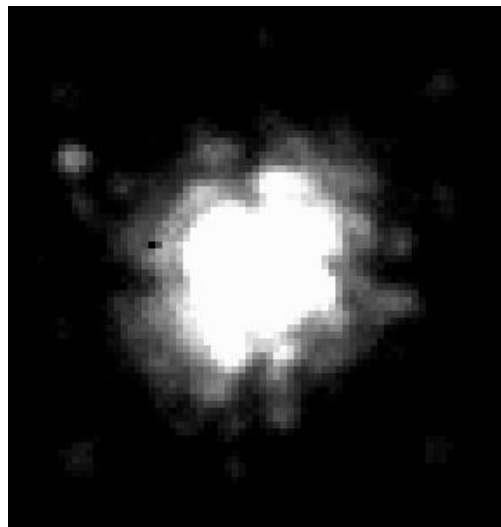


Fig. 11. Through-FQPM image of HD 130948 with our WCS in the K_s band. Note the brown dwarf at 10 o'clock.

4. FUTURE WORK

Another experiment which the WCS makes possible is observation of the expected well-corrected “dark hole” surrounding the central star¹. Normally the diffracted and scattered starlight is too bright for the dark hole to become visible with current generation AO systems. In our case, a Strehl ratio of 0.9 implies a scattered light level, $(1-S)/N^2$, of $\approx 4 \times 10^{-4}$ relative to the star for a 16×16 DM. Normally the innermost stellar diffraction rings would be well above this level, but it is possible to suppress them in a well-corrected image. In particular, one perhaps obvious approach is to make use of the coma aberration, which pushes the light to one side of the geometric image point. As an example, Fig. 1.11 shows the focal plane light distribution resulting from the addition of 1.4 waves of coma to a perfect wavefront. In the cross-cut, it can be seen that all of the diffraction sidelobes on one side of the image are below the 3×10^{-4} level, implying that simply by adding some coma into the adaptive optics DM, a one-sided dark hole of about 4×10^{-4} relative to the star can be produced near the star! Indeed, the four corners of the expected well-corrected square dark-hole region are already evident in Fig. 10. As this phase-aberration-based dark-hole experiment requires no additional hardware whatsoever, it is a very simple and quick approach to demonstrating the dark hole.

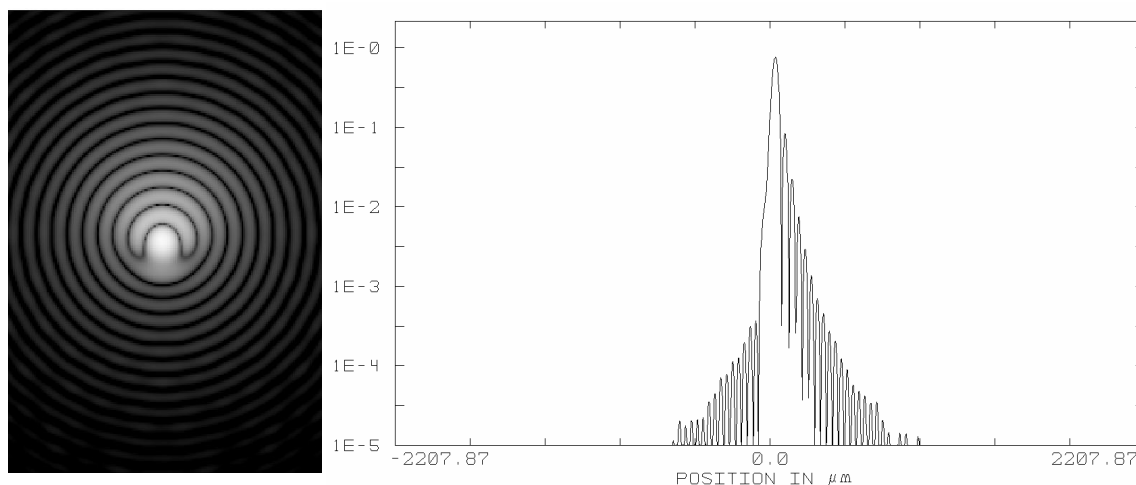


Fig. 12. The use of the coma aberration to produce a dark hole. Left panel: Point spread function for a coma aberration of 1.4 waves. Right panel: vertical cross-cut through the comatic point spread function. Note that all of the sidelobes on the left-hand side of the cross-cut (bottom half of the image) are below 3×10^{-4} .

5. SUMMARY

Using a WCS of diameter 1.5 m on Palomar’s Hale telescope, we have been able to demonstrate many aspects of ExAO including high-Strehl IR ExAO, high stellar rejection with a high-contrast IR coronagraph, and visible AO. Many other experiments are now also possible, such as generation of a dark hole, WFS spatial filtering¹¹, and predictive AO, using the area around the WCS as “forecast” information. The WCS approach thus allows us to demonstrate many of the aspects of ExAO well before next generation ExAO systems come on line.

ACKNOWLEDGEMENTS

This work was carried out at the Jet Propulsion Laboratory, California Institute of Technology, under contract with the National Aeronautics and Space Administration. Observations at the Palomar Observatory were made as part of a continuing collaborative agreement between Palomar Observatory and the Jet Propulsion Laboratory. We wish to thank Rick Burruss and Jeff Hickey and the entire staff of the Palomar 200 inch telescope for their assistance at the Observatory.

REFERENCES

1. F. Malbet, J.W. Yu and M. Shao, *PASP* 107, 386 (1995).
2. A. Sivaramakrishnan, C. Koresko, R.B. Makidon, T. Berkefeld and M.J. Kuchner, *Ap. J.* 552, 397 (2001).
3. P. Riaud, A. Boccaletti, D. Rouan, F. Lemarquis and A. Labeyrie, 2001, *PASP* 113, 1145 (2001).
4. C. Shelton, T. Schneider and S. Baliunas, *Proc. SPIE* 3126, 321 (1997).
5. D. Rouan, P. Riaud, A. Boccaletti, Y. Clenet and A. Labeyrie, *PASP* 112, 1479 (2000).
6. A. Boccaletti et al., *PASP* 116, 1061 (2004).
7. P. Haguenaue et al., *Proc. SPIE* 5905, 261 (2005).
8. P. Haguenaue et al., *Proc. SPIE* 6265 (2006), in press.
9. E. Serabyn et al., in Proc. IAU coll. 200, *Direct Imaging of Exoplanets: Science and Techniques*, Cambridge University, Cambridge, 477 (2006).
10. D. Potter et al., *Ap. J. Lett.* 567, L133 (2002).
11. L.A. Poyneer and B. Macintosh, *J. Opt. Soc. Am.* 21, 810 (2004).